

Received November 26, 2019, accepted December 26, 2019, date of publication January 1, 2020, date of current version January 15, 2020.

Digital Object Identifier 10.1109/ACCESS.2019.2963478

# An Improved Enhancement Algorithm Based on CNN Applicable for Weak Contrast Images

JIAO WANG<sup>ID</sup> AND YANZHU HU<sup>ID</sup>

School of Automation, Beijing University of Posts and Telecommunications, Beijing 100876, China

Corresponding author: Yanzhu Hu (yzhu@263.net)

This work was supported in part by the Subproject of the Key Project of Beijing, China, under Grant Z191100001419001, and in part by the National Natural Science Foundation of China under Grant 61627816.

**ABSTRACT** Image enhancement is commonly used in digital image processing applications. Through image enhancement, the features of the target object are enhanced to make it easier to identify. In order to realize image enhancement, a neural network with a trapezoidal convolution kernel is proposed in this paper. First, weak contrast images are generated using the images in SIDD, DND and RENOIR, which are public datasets used for image denoising. On this basis, pixel distribution characteristics of the R, G and B channels of the weak contrast images are analyzed, and the histogram distribution of the images is given, which can be used to determine the size of the network convolution kernels. Then, a multi-layer convolution neural network is constructed, which uses the original image as an input and outputs the noise map. This network includes convolution kernels of different sizes for the three channels of the original images, and the convolution kernel size is determined by calculating the mean square deviation of the pixels of the corresponding channel. The proposed algorithm provides visually pleasing contrast enhancement. In this paper, a public dataset for image enhancement and actual captured images are separately assessed, both the contrast experiment and ablation experiment results show that the algorithm proposed in this paper can achieve a higher Peak Signal to Noise Ratio (PSNR) and a higher Structural Similarity Index (SSIM) than other image enhancement algorithms.

**INDEX TERMS** Enhancement algorithm, trapezoidal convolution Kernel, image contrast, feature analysis, neural network.

## I. INTRODUCTION

Vision, which uses digital images as the information carrier, accounts for up to 80% of the information that humans receive, thereby making it the main form of information acquisition [1], [2]. However, the quality of digital images usually decreases due to the introduction of noise in such processes as acquisition, transmission, and storage [3]. Image enhancement improves image quality, enriches information, enhances key details, and heightens image interpretation and recognition by highlighting main features and suppressing secondary features [4]. At present, image enhancement is widely used in medical, military, mapping, public security and other fields [5]–[8]. Since it is easy for images to introduce redundant information, which then affects the effect of the image enhancement process, the image enhancement results are often far from satisfactory. Providing an accurate,

reliable, and effective image enhancement algorithm to restore valuable information in images has a wide range of practical applications [9], [10].

In view of the importance of image enhancement technology, a number of image enhancement techniques have been devised. Generally speaking, image enhancement algorithms attempt to structure the optimal mapping between the input image and new level [11]. Image enhancement algorithms can be divided into four categories: image feature-based, visual sense-based, bionic algorithm-based, and neural network-based. Histogram equalization is one of the most typical image contrast enhancement algorithms based on image characteristics, and many researchers have argued that histogram equalization (HE) is a simple and easy method for enhancing the contrast as well as improving image quality [12]. Jasmine et al. used the particle optimization with adaptive cumulative distribution-based histogram enhancement technique (PACDHE) to improve image quality [13]. Satapathy et al. proposed an image contrast

The associate editor coordinating the review of this manuscript and approving it for publication was Ke Gu<sup>ID</sup>.

enhancement algorithm combining various histogram equalization approaches [14]. Singh et al. used an improved contrast-limited adaptive histogram equalization (CLAHE) method to enhance texture features, the contrast, resolvable details, and image structures [15]. As mentioned previously, an algorithm based on histogram equalization can quickly implement image enhancement, and it is usually used for video frame images, but the actual enhancement effect still needs to be improved. An image enhancement algorithm based on visual features is a theoretical computational model of color constancy perception, which is based on the brightness and color perception of human vision. Retinex is one of the most widely used and classical image enhancement algorithms based on visual features [16]. Tang et al. presented an efficient enhancement method for underwater images and videos based on the multi-scale Retinex [17]. Teng et al. estimated the incident component of an image using the multiscale Retinex, which could obtain more edge details and better color fidelity [18]. Sun et al. proposed a new pathological image enhancement method based on the improved single-scale Retinex (SSR) algorithm for medical image processing [19]. Although the Retinex algorithm can effectively enhance images, the computational consumption is considerable. In recent years, with the wider application of bionic algorithms in many areas, these algorithms have also been applied in the image enhancement field. Chen et al. considered image contrast enhancement as an optimization problem and the artificial bee colony (ABC) algorithm was utilized to find the optimal solution for this optimization problem [20]. Prasath et al. proposed a new underwater image enhancement model named the Distance Oriented Cuckoo Search (DOCS) algorithm that included certain phases like contrast correction and color correction [21]. Muniyappan et al. proposed an adaptive genetic algorithm for medical image contrast enhancement [22]. The bionic algorithm can achieve image enhancement quickly and accurately. However, this algorithm is not universal, and its applicability as a single image enhancement algorithm is determined by the specificity of the bionic algorithm and the application scenarios. An image enhancement algorithm based on a convolution neural network is a new kind of intelligent algorithm that has been developed in computer science in recent years. Chen et al. addressed the real time and adaptive problems based on generative adversarial networks (GAN) and proposed a GAN-based restoration scheme (GAN-RS) [23]. Wang et al. proposed a framework called CAENet (convolutional auto-encoder network) which combined a low light processing module with a network training module [24]. Kuang et al. proposed a deep learning method for single infrared image enhancement, and the conditional generative adversarial networks were incorporated into the optimization framework to avoid the background noise being amplified [25]. Liu et al. proposed an underwater image enhancement solution through a deep residual framework to solve the problems of low contrast, blurred details and color distortion of the original underwater images [26]. Ren et al.

proposed a trainable hybrid network to enhance the visibility of degraded images [27]. Furthermore, Szegedy et al. demonstrated that convolution kernels of different sizes can achieve better image recognition results [28].

Inspired by the above algorithms, we proposed an image enhancement algorithm based on a convolutional neural network with a trapezoidal convolution kernel. Through analyzing the characteristics of the R, G, and B channels of weak contrast images, the convolution kernel size of the three channels is determined. On this basis, a convolution neural network that can be easily trained to enhance the image contrast is proposed. The network consists of an up-and down-sampling network. The down-sampling network obtains the feature map of the image by learning a certain association mapping relationship, and the up-sampling network obtains the noise map directly from the feature map through the deconvolution network. By comparing the Peak Signal to Noise Ratio (PSNR) and the Structural Similarity Index (SSIM) of images with the existing image enhancement methods, the results show that the algorithm proposed in this paper based on convolution neural networks with a trapezoidal convolution kernel can obtain better effects and adaptability than other algorithms.

The main work described in the remainder of this paper is as follows. Section 2 introduces the weak contrast image acquisition method based on the public dataset images and analyzes the characteristics of the R, G and B channels of the images so that the convolution kernel sizes of the three channels can be determined. Section 3 introduces the construction method of the convolutional neural network proposed in this paper for image contrast enhancement and the implementation details were given. Section 4 demonstrates the effectiveness of the algorithm proposed in this paper through experiments. In addition, qualitative and quantitative methods are used to evaluate this proposed algorithm and compare it with other image enhancement algorithms. Section 5 presents the conclusions of this paper.

## II. ANALYSIS OF WEAK CONTRAST IMAGES

In this section, we firstly introduce the acquisition method of weak contrast images using the images in the public datasets SIDD, DND and RENOIR. Then, we analyzed the features of the R, G, and B channels of weak contrast images, which can be used to determine the convolution kernel size of the three channels.

### A. METHOD OF GENERATING WEAK CONTRAST IMAGES

The weak contrast image data set is the database of the algorithm proposed in this paper. Considering that the public dataset is not specifically designed for weak contrast image enhancement, we generate weak contrast images based on the original images in the public datasets. With this approach, the generated weak contrast image dataset can be used to analyze the characteristics of the R, G, and B channels of weak contrast images, and it can also be used for the training of the image enhancement network proposed in this paper.

**TABLE 1.** Mean square deviation of the pixels of the R, G, and B channels (Image ID 0537).

AC \ Channel	0	0.1	0.2	0.3	0.4	0.5	0.6	0.7	0.8	0.9
R	67.13	60.88	54.10	47.34	40.56	33.81	27.81	20.06	13.59	6.73
G	72.54	64.77	57.65	50.49	43.16	36.01	28.86	21.71	14.44	7.27
B	73.14	65.99	58.66	51.33	44.01	36.68	29.33	22.01	14.67	7.34

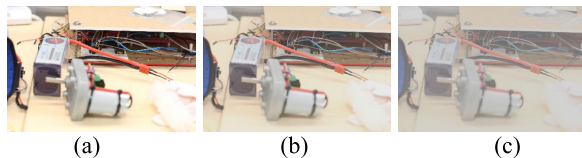


**FIGURE 1.** Demonstration images obtained by changing the attenuation coefficient of the contrast. (a) The image with  $k = 0$  is identical to the original image, (b) the image with  $k = 0.4$  is slightly unclear compared to the original image, and (c) the image with  $k = 0.7$  is obviously blurred due to the decreased contrast.

Generating a weak contrast image means transforming the contrast of an image, which can be achieved by changing the differences between pixels [29-30]. The method that is demonstrated in the following equation is adopted to retain the mean value of the pixel differences between the original image and the generated image.

$$\tilde{P}(i, j) = (1 - k) \cdot (P(i, j) - P_{avg}) + P_{avg} \quad (1)$$

where  $P(i, j)$  is the pixel value of the  $i_{th}$  row in the  $j_{th}$  column in the original image and  $\tilde{P}(i, j)$  is the new value that corresponds to the original image.  $k \in [0, 1]$  is the attenuation coefficient of the contrast, and a larger  $k$  indicates a greater attenuation.  $P_{avg}$  is the mean value of the pixels, which can be computed using the following equation.

$$P_{avg} = (\sum P(i, j)) / n \quad (2)$$

where  $n$  is the number of pixels. The weak contrast images after transformation are given in Fig. 1.

The noise map, which is the difference between weak contrast image and the original image, can be used as the label when training the neural network. The method for generating the noise map is demonstrated in the following equation.

$$\begin{aligned} P_{noisy}(i, j) &= \tilde{P}(i, j) - P(i, j) \\ &= (1 - k)g(P(i, j) - P_{avg}) + P_{avg} - P(i, j) \\ &= k(P_{avg} - P(i, j)) \end{aligned} \quad (3)$$

where  $P_{noisy}(i, j)$  is the value of the  $i_{th}$  row of the  $j_{th}$  column pixel in the noise map, which corresponds to the original image. As the attenuation coefficient increases, the noise becomes increasingly more complex. The noise maps are given in Fig. 2.

Through the method above, we can get weak contrast images with different attenuation coefficients and the corresponding noise maps which can expand the existing data set.

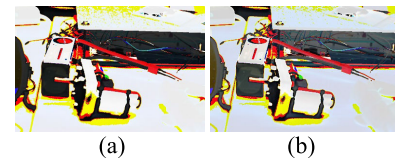


**FIGURE 2.** Demonstration noise maps under different attenuation coefficient. (a) a noise map with an attenuation coefficient of 0.4 and (b) a noise map with an attenuation coefficient of 0.7.

## B. ANALYSIS OF WEAK CONTRAST IMAGES WITH THREE CHANNELS

As previously shown, we can obtain weak contrast images with different attenuation coefficients. Furthermore, we analyze the features of the R, G, and B channels of the weak contrast images. Due to such advantages as image translation, rotation, and zoom invariance, the image histogram is often used to analyze the image features. The histogram can be obtained by equation (4).

$$h(r_k) = n_k \quad (k = 0, 1, \dots, 255) \quad (4)$$

where  $k$  represents the grey level, and  $n_k$  is the number of the pixels in the corresponding level. The normalized histogram can be expressed as follows:

$$p(r_k) = n_k / n \quad (5)$$

where  $n$  indicates the number of pixels, and  $p(r_k)$  is the probability corresponding to each gray level. The sum of all gray level probabilities is 1. By analyzing the characteristics of the R, G, and B channels of the weak contrast images with different attenuation coefficients in the dataset that we mentioned in the previous section, which contains 10,000 images, we find that in the R, G, and B channels, the more discrete the image histogram distribution is, the greater the impact on the channel under different attenuation coefficients (AC) is. In other words, the larger the mean square deviation of the pixels is, the more susceptible the channel is (a histogram is actually a distribution statistic). The mean square deviation of the pixels of the R, G, and B channels of three example images are given in Table 1, Table 2, and Table 3.

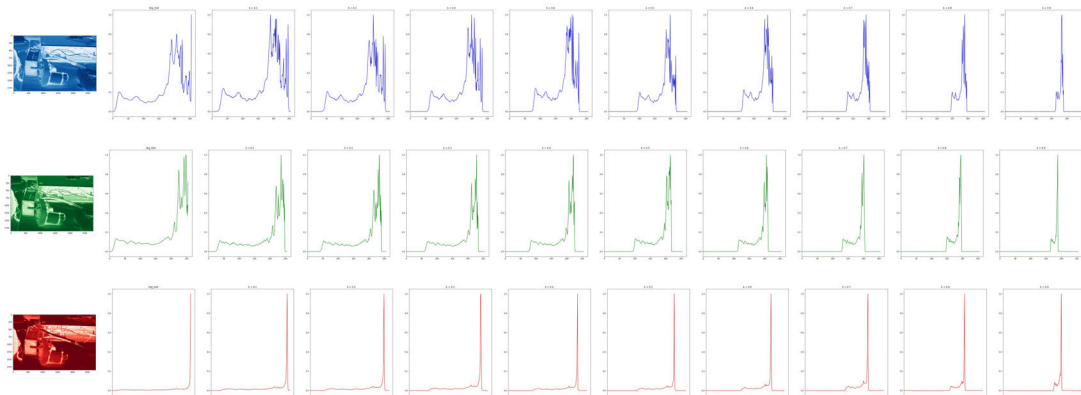
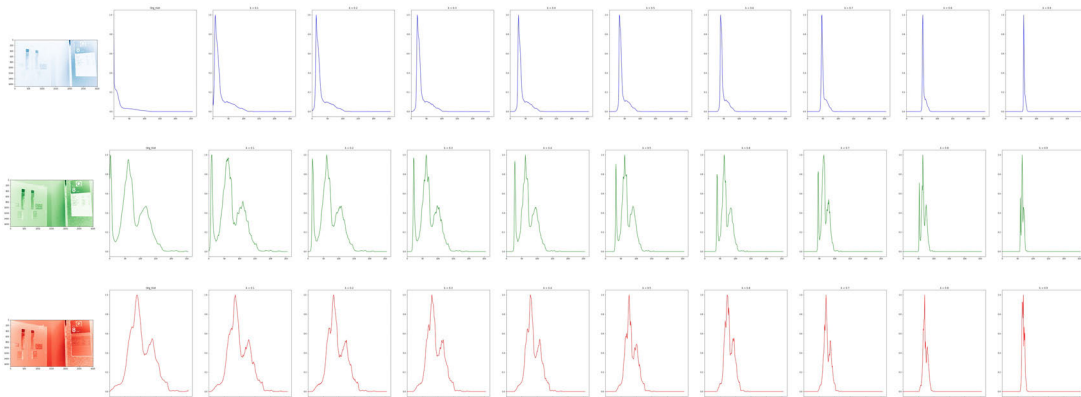
It can be seen from Table 1 that image 0537 has the largest mean square deviation for the B channel, and it is also the most affected as the attenuation coefficient increases. Similarly, as can be seen from Table 2 and Table 3, image 2800 has the largest mean square deviation for the G channel, and image 6633 has the largest mean square deviation for

**TABLE 2.** Mean square deviation of the pixels of the R, G, and B channels (Image ID 2800).

Channel \ AC	0	0.1	0.2	0.3	0.4	0.5	0.6	0.7	0.8	0.9	
Channel	R	36.86	32.91	29.26	25.58	21.94	18.27	14.63	10.90	7.41	3.94
	G	42.43	37.96	33.76	29.52	25.30	21.08	16.85	12.65	8.47	4.23
	B	27.13	24.54	21.87	19.18	16.42	13.69	11.01	8.31	5.61	2.78

**TABLE 3.** Mean square deviation of the pixels of the R, G, and B channels (Image ID 6633).

Channel \ AC	0	0.1	0.2	0.3	0.4	0.5	0.6	0.7	0.8	0.9	
Channel	R	52.86	47.41	42.18	36.93	31.63	26.42	21.08	15.81	10.45	5.30
	G	42.49	38.14	33.87	29.64	25.43	21.21	16.98	12.73	8.49	4.26
	B	39.15	35.04	31.6	27.27	23.37	19.48	15.61	11.69	7.76	3.83

**FIGURE 3.** Histogram of the image 0537. The order is the B channel, G channel and R channel from top to bottom and the attenuation coefficient increases from left to right.**FIGURE 4.** Histogram of the image 2800. The order is the B channel, G channel and R channel from top to bottom and the attenuation coefficient increases from left to right.

the R channel. The specific histogram statistics of the three example images are shown in Fig.3, Fig. 4 and Fig.5.

As can be seen from Fig. 3, the histogram distribution of image 0573 changes more as the attenuation coefficient increases. Channel B is the most affected because of its discrete pixel distribution, which is followed by the G channel and R channel. Similarly, Fig. 4 shows that the G channel

of image 2800 is the most affected and Fig. 5 shows the most affected in image 6633 is the R channel, which are consistent with the mean square deviation. Therefore, in order to adapt to this corresponding characteristic of weak contrast images, we designed convolution kernels with different sizes. Consider that the larger the convolution kernel is, the larger the perceptual field of view. On the contrary, the smaller

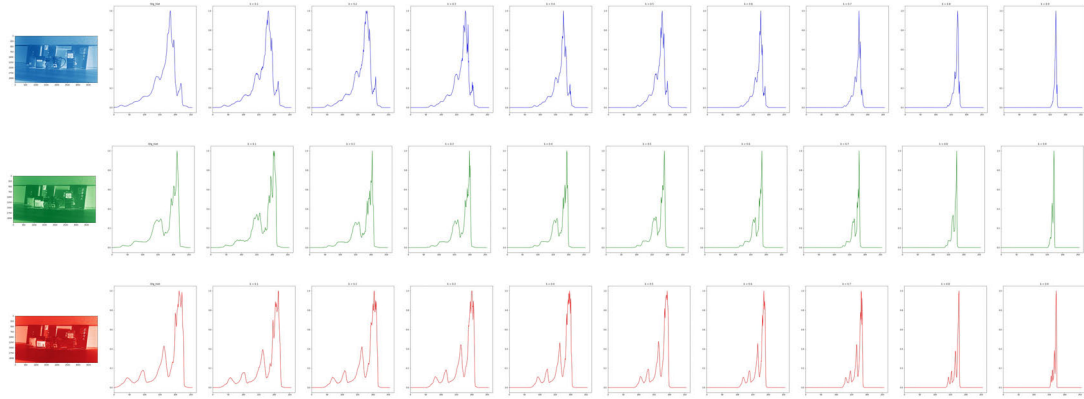


**FIGURE 5.** Histogram of the image 6633. The order is the B channel, G channel and R channel from top to bottom and the attenuation coefficient increases from left to right.

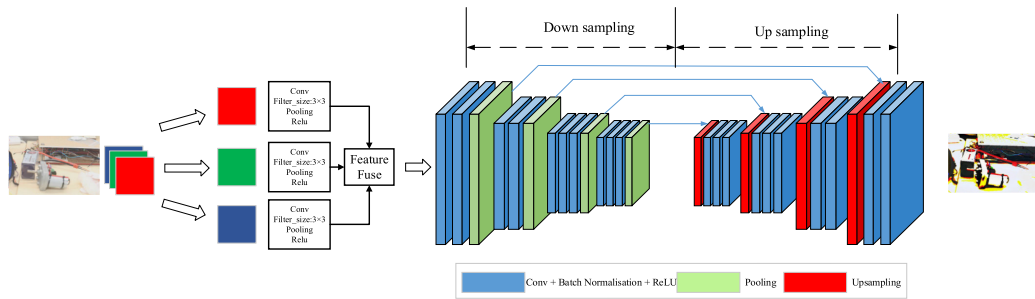


**FIGURE 6.** Architecture of the proposed network, which consists of a down-sampling and up-sampling network.

the convolution kernel is, the easier it can be to see detailed features. The specific size of the convolution kernel is determined in Section 3.

### III. WEAK CONTRAST IMAGE ENHANCE NETWORK

In this section, we first introduce the layer design of the proposed neural network with different sized convolution kernels to realize image enhancement. Then, we present the implementation details of our neural network.

#### A. ESTABLISHMENT OF THE NEURAL NETWORK

The establishment of this network that contains down- and up-sampling is completely influenced by the successful application of deep learning in the machine vision field [31]–[37]. The network realizes image contrast enhancement by learning some mapping relationships between the input images and the noise maps. Considering the weak representation ability of a shallow network, it is necessary to increase the network depth [38]–[43]. However, as the network depth increases, the difficulty of network training will increase, as well. In full consideration of this difficulty, a multi-layer convolution network is chosen to build the network, which can reduce the difficulty of training and increase the network representation ability. The structure of the neural network is shown in Fig. 6.

As can be seen in Fig. 6, the network proposed in this paper has two parts: a down-sampling network and an up-sampling

network. The down-sampling network consists of two layers: a feature extraction layer and a characteristic activation layer. Through the two layers, the non-linear features of the weak contrast images are extracted. However, the size of the feature map extracted by the down-sampling network is smaller than that of the original image; thus, the up-sampling network is used to make the feature map the same size as the original image. The up-sampling network also contains two layers, a high dimensional mapping layer and an image generation layer, and both of the two layers can increase the size of the feature map. Through the four layers, we can get the noise map. Then, the construction of each layer is explained separately.

#### 1) FEATURE EXTRACTION LAYER

To learn the relationship between input images and noise maps, we first extract the R, G and B channels, which are the primary colors of each input image. The convolution kernel sizes of the three channels are set, and each channel uses a high-dimensional vector. It can be expressed as follows:

$$\begin{aligned} & \text{out}_{R1}(N_i, C_{outR}) \\ &= \text{bias}_{R1}(C_{outR}) + \sum_{k=0}^{C_{inR}-1} \text{weight}_{R1}(C_{outR}, k) \cdot \text{input}_{R1}(N_i, k) \end{aligned} \quad (6)$$

where  $N_i$  is the batch size,  $out_{R1}$  represents the convolution output of the R channel, and  $bias(\cdot)$  represents a paranoid vector.  $C_{inR}$  means the R channel of the image.  $k$  is the number of times a graph must be convoluted.  $weight(\cdot)$  represents the weight of the input to the output, which is a parameter that needs to be trained.  $input(\cdot)$  represents the image that is input into the convolution kernel, and  $\cdot$  is the valid 2D cross-correlation operator. Similarly, we can define the feature extraction formulas of the G channel and B channel.

The largest convolution kernel size is defined as  $7 \times 7$ , which is used to feel the global change. The middle size of the convolution kernel is  $5 \times 5$  and the smallest size is  $3 \times 3$ , which is used to perceive the details. Each channel is assigned a different sized convolution kernel based on its mean square deviation. In the interest of making the output of the R, G and B channels have the same size, the zero-padding method is adopted, and the moving step of the convolution kernel is set as 1. The Rectified Linear Unit (ReLU) is used as the activation function.

## 2) CHARACTERISTIC ACTIVATION LAYER

Inspired by the feature enhancement layer in [44], a feature activation layer is established in this paper. Considering that the weak edge information in the feature graph is easily ignored, we map the acquired features of the last layer to a more sensitive feature space through the convolution network of this activation layer, which can get more edge information and increase the nonlinear characteristics of the network. The feature activation layer can be expressed as follows:

$$\begin{aligned} & out_{R2}(N_i, C_{outR}) \\ &= bias_{R2}(C_{outR}) + \sum_{k=0}^{C_{outR}-1} weight_{R2}(C_{outR}, k) \cdot out_{R1}(N_i, C_{outR}) \end{aligned} \quad (7)$$

where  $out_{R2}$  represents the activation layer output of the R channel, and the Rectified Linear Unit (ReLU) is used as the activation function.

In the same way, we can define the characteristic activation formulas of the G channel and B channel.

## 3) HIGH DIMENSIONAL MAPPING LAYER

By mapping from one high dimension vector to another high dimensional vector, the high dimensional mapping layer increases the nonlinear characteristics of the network, which can increase the network's expression and make it easier for the network to converge. The high dimensional mapping layer can be expressed as follows:

$$\begin{aligned} & out_{R3}(N_i, C_{outR}) \\ &= bias_{R3}(C_{outR}) + \sum_{k=0}^{C_{outR}-1} weight_{R3}(C_{outR}, k) \cdot out_{R2}(N_i, C_{outR}) \end{aligned} \quad (8)$$

where  $out_{R3}$  represents the activation layer output of the R channel, and the Rectified Linear Unit (ReLU) is used as the activation function.

By the same token, we can define the high dimensional mapping formulas of the G channel and B channel.

## 4) IMAGE GENERATION LAYER

Through the convolution layer above, the output of each channel has multiple maps. In order to get the pixel value of the R, G, and B channels of the enhanced images, the final image generation network needs to be defined as follows:

$$\begin{aligned} & out_{R4}(N_i, C_{outR}) \\ &= bias_{R4}(C_{outR}) + \sum_{k=0}^{C_{outR}-1} weight_{R4}(C_{outR}, k) \cdot out_{R3}(N_i, C_{outR}) \end{aligned} \quad (9)$$

where  $out_{R4}$  represents the activation layer output of R channel. The image generation formulas of the G channel and B channel can be define by the same token.

In the whole network, the weight of every layer  $\{weight_1, weight_2, weight_3, weight_4\}$  and the paranoid vector  $\{bias_1, bias_2, bias_3, bias_4\}$  are unknown. Those unknown parameters can be achieved by minimizing the Mean Squared Error (MSE) loss function, which is expressed as follows:

$$L(\Theta) = \frac{1}{N} \sum_{i=1}^N \|F(P_i; \Theta) - nos\mu_i\|^2 \quad (10)$$

where  $N$  is the number of images in a training batch,  $\Theta$  is a collection of all unknown parameters,  $P_i$  is the weak contrast image,  $nos\mu_i$  is the noise map that corresponds to  $P_i$ , and  $F$  is the learned mapping function. The purpose of the training network is to minimize  $L(\Theta)$ . In this paper, the BP network is used to train our network.

## B. IMPLEMENT DETAILS OF THE PROPOSED NETWORK

Our model is implemented using the Pytorch package [45], and the network parameter settings are shown in Table 4. In the initial stage, the parameters of the network are randomly generated by the function, and the paranoid vector is set as zero. The learning rate is 0.05, which declines by 0.3 every 5000 iterations, and the batch size is 16. The model is trained on a computer with an Intel(R) Xeon(R) CPU E5-2670@2.30GHz and an NVIDIA GeForce GTX 1080.

Through the method above, we can get a noise map that is the same size as the original image. By subtracting the noise map from the weak contrast image, we can get the enhanced image.

## IV. EXPERIMENTAL RESULTS

In this section, we will comprehensively evaluate the performance of the algorithm proposed in this paper. Firstly, the trained network is used to obtain the noise map such that the enhanced image can be obtained. The image verifies the feasibility of the network and that it achieves good visual

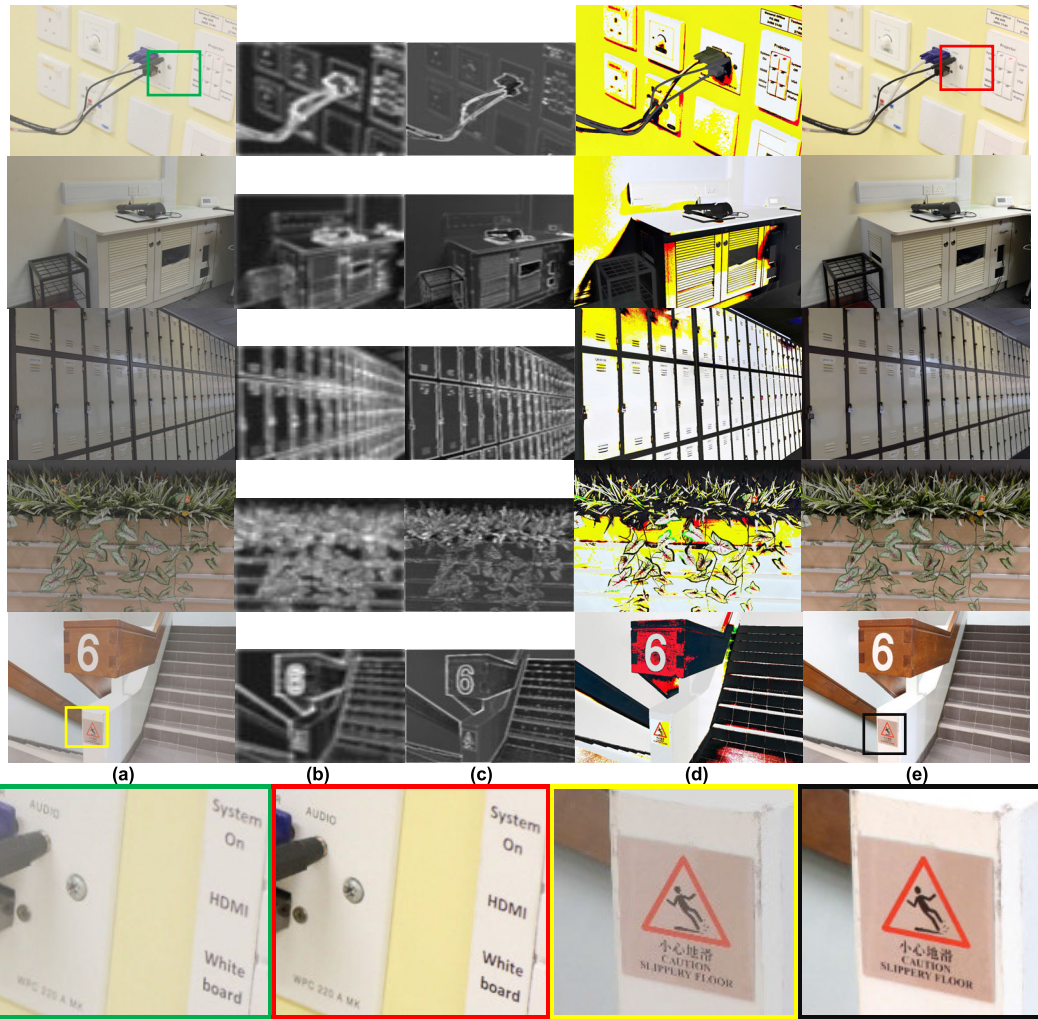


**FIGURE 7.** Enhancement effects of different images. (a) Generated weak contrast images, (b) extracted feature maps, (c) enhanced feature maps, (d) Up-sampled noise maps and (e) enhanced images.

**TABLE 4.** Parameter settings of the network.

Formulation	Kernel size	Number	Padding
Feature extraction layer	3×3 (smallest channel)	32	1
	5×5 (middle channel)	32	2
	7×7 (largest channel)	32	3
Characteristic activation layer	32×5×5 (3 channels)	16	2
High dimensional mapping layer	16×3×3 (3 channels)	8	2
Image generation layer	8×3×3 (3 channels)	1	1

results. Then, quantitative methods are used to demonstrate the advantages of the proposed algorithm through comparing the Peak Signal to Noise Ratio (PSNR) and Structural Similarity Index (SSIM) of images with those of other two kinds of widely used algorithms: one is traditional image enhancement algorithms based on parameters, such as the CLAHE (Contrast-Limited Adaptive Histogram Equalization) algorithm [15], the SSR (Single-Scale Retinex) algorithm [19],

the ABC (Artificial Bee Colony) algorithm[20] and the DOCS (Distance Oriented Cuckoo Search) algorithm[21], and the other is deep learning based image enhancement algorithms, for instance the CAEN (Convolutional Auto-encoder Network) algorithm[24], the DCNN (Deep Convolutional Neural Networks) algorithm [25], the DRF (Deep Residual Framework )algorithm [26] and DHN (Deep Hybrid Network) algorithm[27]. In addition, an ablation experiment on the convolution kernel size is conduct to indicate the advantage of proposed network in this paper. At last, the real weak contrast images that captured actually are used for experimental comparisons and satisfactory results are obtained.

#### A. FEASIBILITY EVALUATION OF THE MODEL

Based on the basic network parameter settings in Table 4, we evaluate the feasibility of the built network. The data set is formed using the method mentioned before. We select five images to show the effect of the network, and the results are shown in Fig.7.

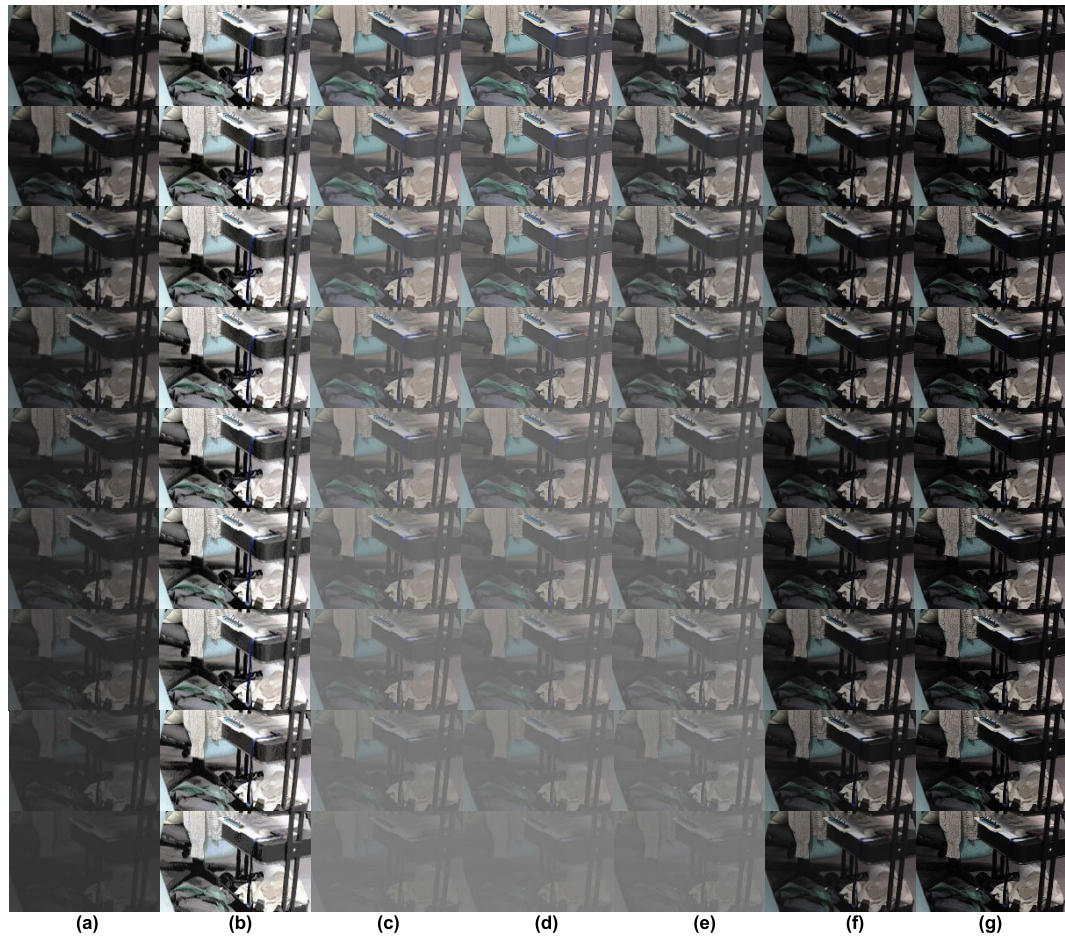


**FIGURE 8.** Enhanced images of different algorithms, and the attenuation coefficient from top to bottom increases from 0.1 to 0.9. (a) Weak contrast images with different attenuation coefficients, (b) enhanced images using CLAHE, (c) enhanced images using SSR, (d) enhanced images using ABC, (e) enhanced images using DOCS, (f) enhanced images using our method and (g) original images.

As shown in Fig. 7, the proposed algorithm can enhance weak contrast images and achieve satisfactory visual effects. The comparison and analysis of the results obtained by this method with those of other algorithms are put in the next section.

#### B. COMPARISON AND ANALYSIS OF DIFFERENT ALGORITHMS ON GENERATED IMAGES

In this part, we will compare the performance of our algorithm using a trapezoidal convolution kernel with other algorithms. Firstly, we select a weak contrast image with different attenuation coefficients for the comparison experiments. Fig. 8 shows the enhanced images obtained by traditional image enhancement algorithms.

As shown in Fig. 8, different enhancement algorithms have different enhancement effects. The CLAHE algorithm can significantly enhance the image contrast under different attenuation coefficients but it will cause image distortions. The SSR algorithm can make the image conform to human visual habits by enhancing the brightness of the image when the attenuation coefficient is low. However,

the contrast of the image cannot be substantially improved while the attenuation coefficient increases. The enhancement effect of the ABC algorithm on the weak contrast image is general, regardless of the attenuation coefficient. The DOCS algorithm can achieve image enhancement to a certain extent when the attenuation coefficient is low, but it cannot achieve image enhancement when the attenuation coefficient increases. Fig. 9 is the enhanced images obtained by deep learning based image enhancement algorithms.

As shown in Fig. 9, for the images with different attenuation coefficients, the CAEN algorithm has the same enhancement effect, which is linear. The enhancement of the DCNN algorithm is comparable to the CAEN algorithm, and when the attenuation coefficient increases, the enhancement is not satisfactory. The DRF gets the worst enhancement and it has almost no effect on the images with high attenuation coefficient. The enhancement of the DHN algorithm is improved compared with the above three algorithms, but the effect is not significant. Compared with other deep learning based image enhancement algorithms, the network proposed in this

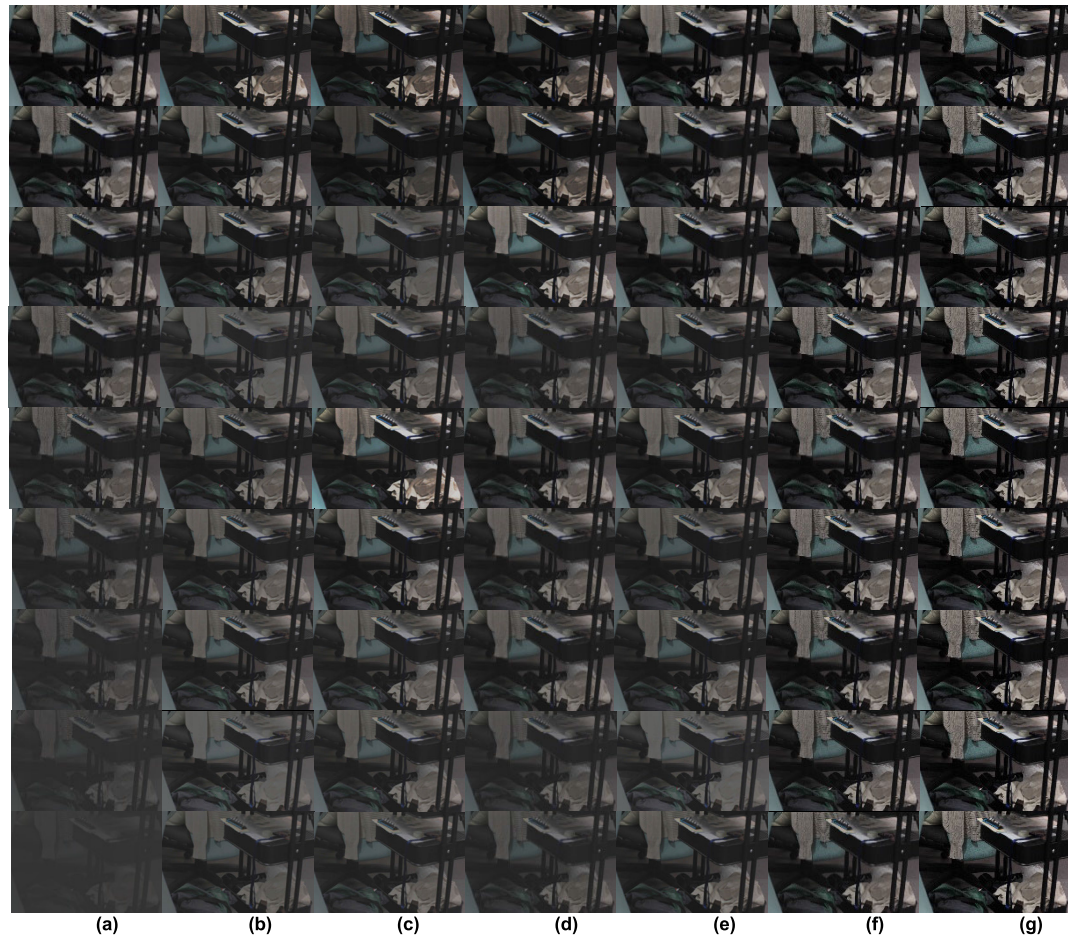


**FIGURE 9.** Enhanced images of different algorithms, and the attenuation coefficient from top to bottom increases from 0.1 to 0.9. (a) Weak contrast images with different attenuation coefficients, (b) enhanced images using CAEN,(c) enhanced images using DCNN,(d) enhanced images using DRF, (e) enhanced images using DHN, (f)enhanced images using our method, and (g) original images.

paper has a good enhancement effect whether the attenuation coefficient is high or not.

In order to further illustrate the effect of the algorithm proposed in this paper, we select some images from the dataset that have the same attenuation coefficient for experimentation and the results are shown in Fig. 10.

As shown in Fig.10, the conclusion is the same as that in Fig. 8. The CLAHE algorithm will create some distortion when enhancing the image under any circumstances. The SSR algorithm can effectively improve the brightness of the image, but the contrast enhancement effect is general. The ABC and DOCS algorithms are not ideal for enhancing the contrast of images. Compared with other algorithms, the algorithm proposed in this paper can effectively enhance the image and avoid distortion. Fig. 11 shows the enhanced images obtained by deep learning based image enhancement algorithms.

As can be seen in Fig. 11 that the DRF algorithm gets the worst enhancement while the DHN gets the best among the four deep learning based image enhancement algorithms, which are consistent with those in Fig. 9. Compared with other algorithms, the algorithm proposed in this paper can

not only enhance weak contrast images but also enhance images in common scenes effectively. In the next section, the ablation experiments on the network proposed in this paper are conducted.

### C. ABLATION EXPERIMENT ON THE CONVOLUTION KERNEL SIZE

In this part, in order to evaluate the network improvement brought by different convolution kernel sizes, we have built other six networks: (a) a network with the same convolution kernel size of  $3 \times 3$ , (b) a network with the same convolution kernel size of  $5 \times 5$ , (c) a network with the same convolution kernel size of  $7 \times 7$ , (d) a network with convolution kernel size of  $3 \times 3, 5 \times 5$  and  $5 \times 5$ , (e) a network with convolution kernel size of  $3 \times 3, 7 \times 7$  and  $7 \times 7$ .(f) a network with convolution kernel size of  $5 \times 5, 5 \times 5$  and  $7 \times 7$ . By comparing the network proposed in this article compared with the networks mentioned above, the advantages of the proposed network are verified. Fig. 12 shows the enhanced images with different attenuation coefficients obtained by the networks with different structures.

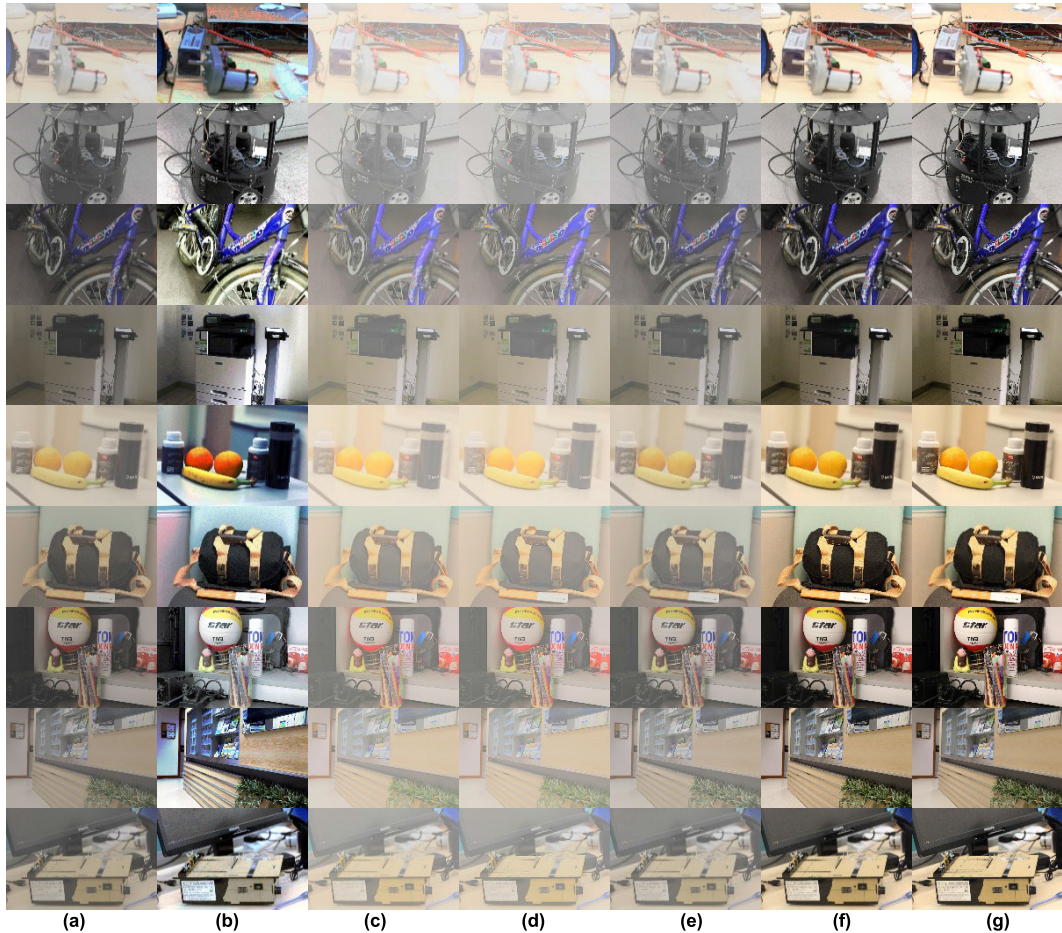


**FIGURE 10.** Enhanced images of different algorithms with the same attenuation coefficient. (a) Different weak contrast images with the same attenuation coefficient, (b) enhanced images using CLAHE, (c) enhanced images using SSR, (d) enhanced images using ABC, (e) enhanced images using DOCS, (f) enhanced images using our method, and (g) original images.

It can be seen from Fig.12 that the networks with different convolution kernel sizes have different sensitivity to the images with different attenuation coefficients. For the images with a lower attenuation coefficient (e.g. the attenuation coefficient is 0.1 or 0.2), the enhancement effect of the networks with different convolution kernel sizes is similar. As the attenuation coefficient increases, the network with a smaller convolution kernel pays more attention to the details of the images and effectively enhances the contrast. But it also introduces noise with a slight distortion. On the contrary, the network with a larger convolution kernel has a better overall enhancement effect, while the detail enhancement is neglected and the contrast enhancement effect is general. Especially when the attenuation coefficient increases to 0.9, the enhancement effect of the network with the largest convolution kernel is not ideal. The analysis of the enhancement effects of different images is following and Fig.13 is a representation of different images obtained by different networks.

It can be seen in Fig.13 that the network with the same convolution kernel size of  $3 \times 3$  increases effectively the contrast of different images while the network with the same

convolution kernel size of  $7 \times 7$  improves the brightness of the images. The algorithm proposed in this paper has a better visual enhancement effect that can effectively enhance the image and also take into account the image details and the qualitative comparison and analysis of the proposed algorithms are put in the next section.

#### D. QUANTITATIVE COMPARISON AND ANALYSIS OF DIFFERENT ALGORITHMS

In this part, we will quantitatively evaluate the performance of the algorithm by calculating the Peak Signal to Noise Ratio (PSNR) and the Structural Similarity Index (SSIM) of the enhanced images. The PSNR and SSIM are two common indicators for evaluating image quality. The PSNR is based on communication theory, and it is the ratio of the maximum semaphore to the noise intensity. Since digital images represent image pixels in discrete numbers, the maximum pixel value of the image is used instead of the maximum semaphore. The specific formula is as follows:

$$PSNR = 10 \times \lg \frac{L \times L}{MSE} \quad (11)$$

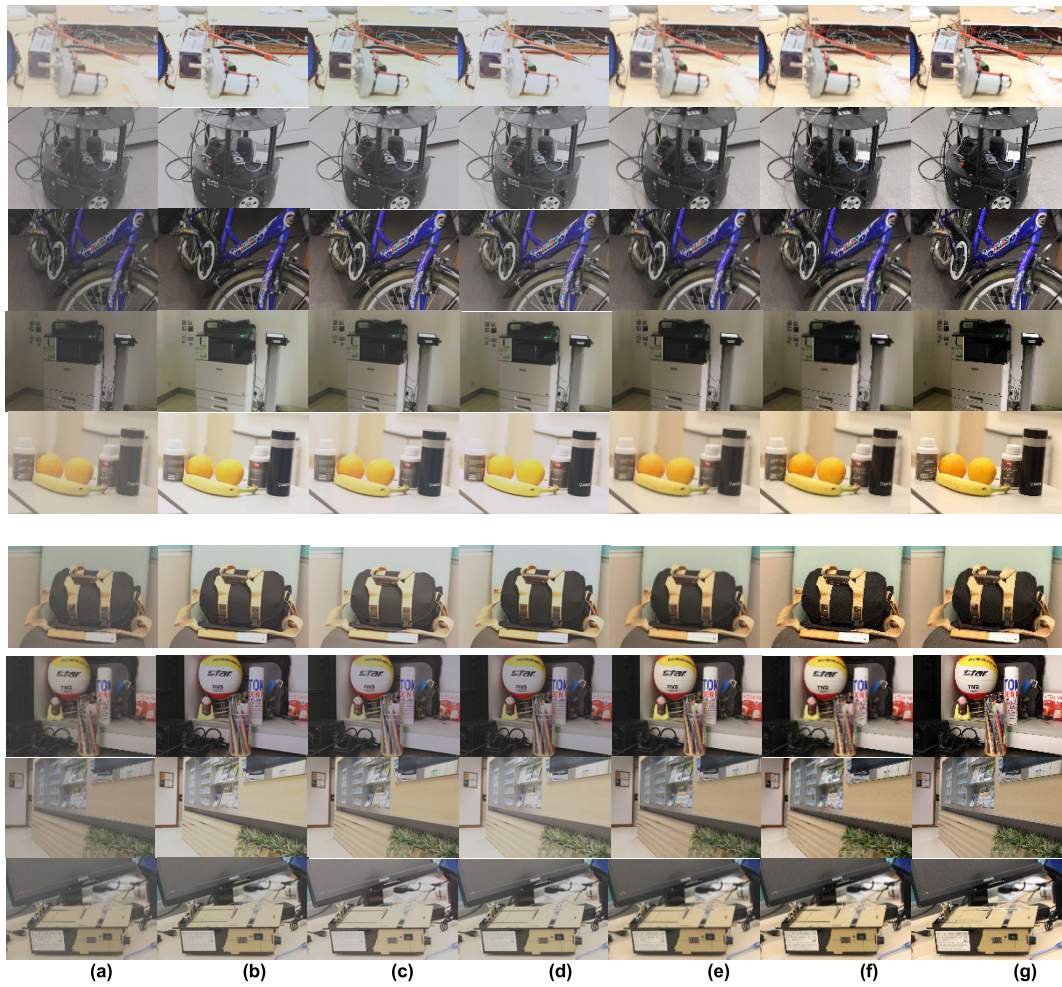


**FIGURE 11.** Enhanced images of different algorithms with the same attenuation coefficient. (a) Weak contrast images with different attenuation coefficients, (b) enhanced images using CAEN, (c) enhanced images using DCNN, (d) enhanced images using DRF, (e) enhanced images using DHN, (f) enhanced images using our method and (g) original images.

**TABLE 5.** the Peak Signal to Noise Ratio (PSNR) of the enhanced images with different attenuation coefficients using various algorithms.

AC	CLAHE	SSR	ABC	DOCS	CAEN	DCNN	DRF	DHN	Our algorithm
0.1	28.82	31.41	27.83	26.96	32.68	32.65	32.46	33.06	33.87
0.2	28.78	31.16	27.75	26.89	32.63	32.61	32.42	33.01	33.79
0.3	28.73	30.91	27.65	26.80	32.58	32.56	32.37	32.95	33.70
0.4	28.69	30.65	27.51	26.71	32.54	32.51	32.32	32.87	33.59
0.5	28.66	30.39	27.36	26.6	32.47	32.45	32.27	32.78	33.46
0.6	28.63	30.12	27.20	26.49	32.42	32.39	32.22	32.70	33.31
0.7	28.61	29.81	27.03	26.39	32.34	32.32	32.17	32.61	33.13
0.8	28.59	29.49	26.85	26.28	32.27	32.24	32.11	32.52	32.91
0.9	28.58	29.19	26.67	26.17	32.18	32.16	32.04	32.41	32.63

where  $L$  is the maximum gray value of the pixels in the image, which is generally 255; and  $MSE$  is the mean square deviation of an image. The MSE of an image can be calculated as follows:

$$MSE = \frac{1}{M \times N} \sum_{0 \leq i < N} \sum_{0 \leq j < M} (f_{ij} - f'_{ij})^2 \quad (12)$$

where  $M$  and  $N$  respectively represent the length and width of the image,  $f_{ij}$  represents the gray value of point  $(i, j)$  in the original image, and  $f'_{ij}$  represents the pixel value of point  $(i, j)$  in the image after segmentation. The Peak Signal to Noise Ratio (PSNR) of an image with different attenuation coefficients are given in Table 5 while the Peak Signal to Noise Ratio (PSNR) of different enhanced images using various algorithms are given in Table 6.



**FIGURE 12.** Enhanced images using deep neural networks with different convolution kernel sizes, and the attenuation coefficient from top to bottom increases from 0.1 to 0.9. (a) Weak contrast images with different attenuation coefficients, (b) enhanced images using a network with the same convolution kernel size of  $3 \times 3$ , (c) enhanced images using a network with the same convolution kernel size of  $5 \times 5$ , (d) enhanced images using a network with the same convolution kernel size of  $7 \times 7$ , (e) enhanced images using a network with the same convolution kernel size of  $3 \times 3, 5 \times 5$  and  $5 \times 5$ , (f) enhanced images using a network with the same convolution kernel size of  $3 \times 3, 7 \times 7$  and  $7 \times 7$ , (g) enhanced images using a network with the same convolution kernel size of  $5 \times 5, 5 \times 5$  and  $7 \times 7$ , (h) enhanced images using the network proposed in this paper.

**TABLE 6.** The Peak Signal to Noise Ratio (PSNR) of the enhanced images with different attenuation coefficients using the networks with different convolution kernel sizes.

AC	Convolution kernel sizes	3×3	5×5	7×7	3×3	3×3	5×5	3×3
		3×3	5×5	7×7	5×5	7×7	5×5	5×5
		3×3	5×5	7×7	5×5	7×7	7×7	7×7
0.1		33.81	33.83	33.81	33.88	33.87	33.79	33.87
0.2		33.65	33.66	33.67	33.72	33.72	33.71	33.79
0.3		33.56	33.55	33.56	33.62	33.62	33.62	33.70
0.4		33.43	33.45	33.45	33.47	33.49	33.50	33.59
0.5		33.32	33.34	33.34	33.39	33.37	33.37	33.46
0.6		33.16	33.17	33.16	33.22	33.22	33.21	33.31
0.7		32.97	32.98	32.98	33.02	33.03	33.03	33.13
0.8		32.75	32.75	32.76	32.81	32.80	32.80	32.91
0.9		32.45	32.43	32.45	32.49	32.49	32.51	32.63

It can be seen from Table 5 that for images with different attenuation coefficients, the Peak Signal to Noise Ratio (PSNR) does not change much when enhancing the

images using the CLAHE algorithm. However, since the image is distorted, the PSNR is smaller than that of the SSR algorithm. The SSR algorithm achieves a larger PSNR by



**FIGURE 13.** Enhanced images using deep neural networks with different convolution kernel sizes. (a) Different weak contrast images, (b) enhanced images using a network with the same convolution kernel size of  $3 \times 3$ , (c) enhanced images using a network with the same convolution kernel size of  $5 \times 5$ , (d) enhanced images using a network with the same convolution kernel size of  $7 \times 7$ , (e) enhanced images using a network with the same convolution kernel size of  $3 \times 3, 5 \times 5$  and  $5 \times 5$  (f) enhanced images using a network with the same convolution kernel size of  $3 \times 3, 7 \times 7$  and  $7 \times 7$  (g) enhanced images using a network with the same convolution kernel size of  $5 \times 5, 5 \times 5$  and  $7 \times 7$  (h) enhanced images using the network proposed in this paper.

enhancing the brightness of the image, but it decreases rapidly when the attenuation coefficient increases. The ABC and DOCS algorithms get a smaller PSNR because of their general image enhancement effects. The CAEN algorithm can get a higher PSNR than other traditional image enhancement algorithms, of which the enhancement effect is the same with DCNN algorithm. The DRF algorithm has the worst enhancement compared with other deep learning based enhancement algorithms and the enhancement becomes worse as the attenuation coefficient increases. The DHN algorithm can get the second highest PSNR than other algorithms and it has a good enhancement effect. On the whole, the algorithm proposed in this paper can obtain the highest PSNR, which means that the algorithm proposed in this paper has the best enhancement effect compared with those of other algorithms.

As shown in Table 6, for the images with different attenuation coefficient, the networks with different convolution kernel sizes have a better enhancement effects than these with

the same convolution kernel sizes, meaning that the network of which the convolution kernels of different sizes can achieve better image enhancement effects.

As shown in Table 7, for different enhanced images, the algorithm proposed in this paper can obtain the highest PSNR, which means that the proposed algorithm has the best enhancement effect in any case

It can be seen from Table 8 that for different images the networks with different convolution kernel sizes can obtain a higher PSNR compared with other networks. What's more, the network with the same convolution kernel size of  $3 \times 3$  gets the smallest PSNR, which means that the network introduces noise although the contrast is enhanced.

The Structural Similarity Index (SSIM) is another indicator that measures the similarity of two images. The method was first proposed by the University of Texas at Austin's Laboratory for Image and Video Engineering. If there are two images, one after enhancement and the other before enhancement, the SSIM can be used to evaluate the

**TABLE 7.** The Peak Signal to Noise Ratio (PSNR) of different enhanced images using various algorithms.

Image ID	CLAHE	SSR	ABC	DOCS	CAEN	DCNN	DRF	DHN	Our algorithm
0537	26.81	32.14	27.45	27.26	33.21	33.16	32.96	33.73	33.97
1077	28.15	31.78	27.93	27.03	33.69	32.65	32.53	33.33	33.56
1618	26.98	31.13	26.70	26.75	32.26	32.21	31.96	32.72	32.78
1723	27.46	31.01	26.77	26.87	32.01	31.94	31.76	32.58	32.89
7222	27.23	31.97	27.80	27.48	33.02	32.96	32.75	33.55	33.89
8310	27.54	31.94	27.89	27.18	32.98	32.93	32.70	33.51	33.71
8595	27.24	31.12	27.21	26.63	32.23	32.18	31.93	32.71	33.15
9365	26.88	31.33	26.81	27.44	32.28	32.25	32.08	32.89	33.38
9452	27.80	31.62	27.12	27.02	32.60	32.56	32.38	33.19	33.58

**TABLE 8.** The Peak Signal to Noise Ratio (PSNR) of different enhanced images using the networks with different convolution kernel sizes.

Image ID	Convolution	3×3	5×5	7×7	3×3	3×3	5×5	3×3
	kernel size	3×3	5×5	7×7	5×5	7×7	5×5	5×5
		3×3	5×5	7×7	5×5	7×7	7×7	7×7
0537		33.79	33.84	33.81	33.88	33.87	33.91	33.97
1077		33.38	33.43	33.42	33.49	33.49	33.50	33.56
1618		32.59	32.64	32.62	32.71	32.70	32.72	32.78
1723		32.71	32.75	32.74	32.81	32.82	32.82	32.89
7222		33.75	33.78	33.77	33.82	33.83	33.82	33.89
8310		33.51	33.55	33.53	33.64	33.65	33.65	33.71
8595		32.98	33.03	33.02	33.07	33.09	33.08	33.15
9365		33.21	33.26	33.24	33.31	33.32	33.31	33.38
9542		33.41	33.46	33.46	33.52	33.53	33.51	33.58

**TABLE 9.** The Structural Similarity Index (SSIM) of the enhanced images with different attenuation coefficients using various algorithms.

AC	CLAHE	SSR	ABC	DOCS	CAEN	DCNN	DRF	DHN	Our algorithm
0.1	0.88	0.81	0.77	0.71	0.87	0.86	0.85	0.89	0.94
0.2	0.87	0.78	0.75	0.68	0.84	0.85	0.83	0.87	0.93
0.3	0.85	0.73	0.72	0.64	0.81	0.81	0.79	0.84	0.92
0.4	0.83	0.67	0.67	0.60	0.78	0.77	0.76	0.80	0.90
0.5	0.80	0.61	0.61	0.54	0.72	0.73	0.70	0.75	0.88
0.6	0.77	0.53	0.52	0.47	0.65	0.66	0.62	0.69	0.86
0.7	0.74	0.45	0.42	0.38	0.57	0.58	0.54	0.62	0.83
0.8	0.70	0.36	0.29	0.29	0.49	0.50	0.45	0.54	0.79
0.9	0.65	0.25	0.16	0.17	0.41	0.40	0.35	0.46	0.75

enhancement effect. The calculation formula is as follow:

$$SSIM(I_O, I_S) = \frac{(2\mu_{I_O}\mu_{I_S} + c_1)(2\sigma_{I_O}\sigma_{I_S} + c_2)}{(\mu_{I_O}^2 + \mu_{I_S}^2 + c_1)(\sigma_{I_O}^2 + \sigma_{I_S}^2 + c_2)} \quad (13)$$

where  $I_O$  represents the original image, and  $I_S$  represents the enhanced image.  $\mu_{I_O}$  and  $\mu_{I_S}$  respectively represent the mean values of images  $I_O$  and  $I_S$ ;  $\sigma_{I_O}$  and  $\sigma_{I_S}$  represent the standard deviations of images  $I_O$  and  $I_S$ , respectively;  $\mu_{I_O}^2$  and  $\mu_{I_S}^2$  are the squares of  $\mu_{I_O}$  and  $\mu_{I_S}$ , respectively;  $\sigma_{I_O}^2$  and  $\sigma_{I_S}^2$  represent the variance of images  $I_O$  and  $I_S$ , respectively;  $c_1$  and  $c_2$  are the constants that maintain stability in order to prevent the denominator from being zero. Normally,  $c_1 = (K_1 * L)^2$  and  $c_2 = (K_2 * L)^2$ , where  $K_1 = 0.01$  and  $K_2 = 0.03$ , respectively.  $L$  is the dynamic range of pixel values, and it is generally set as 255. The Structural Similarity Index (SSIM) of an image under different attenuation coefficients are given

in Table 7 and the Structural Similarity Index (SSIM) of different enhanced images using various algorithms are given in Table 8.

As shown in Table 9, for images with different attenuation coefficients, the larger the attenuation coefficient is, the smaller the SSIM is, and the worse the enhancement result is. When the CLAHE algorithm enhances the image, the SSIM does not change significantly. The SSIM obtained by the SSR algorithm are significantly different, which means that it is not adaptable to the attenuation coefficient and it has weak robustness. The SSIM obtained by the ABC and this by the DOCS algorithms are comparable; meanwhile, the enhancement effects of these two algorithms are not good. The CAEN algorithm and the DCNN algorithm can get a larger SSIM than other traditional image enhancement algorithms, which is consistent with these in Table 5. The DRF algorithm gains

**TABLE 10.** The Structural Similarity Index (SSIM) of the enhanced images with different attenuation coefficients using the networks with different convolution kernel sizes.

Convolution kernel size	$3 \times 3$	$5 \times 5$	$7 \times 7$	$3 \times 3$	$3 \times 3$	$5 \times 5$	$3 \times 3$
AC	$3 \times 3$	$5 \times 5$	$7 \times 7$	$5 \times 5$	$7 \times 7$	$5 \times 5$	$5 \times 5$
0.1	0.92	0.92	0.91	0.92	0.92	0.93	0.94
0.2	0.91	0.91	0.90	0.91	0.90	0.91	0.93
0.3	0.89	0.88	0.88	0.89	0.88	0.89	0.92
0.4	0.85	0.86	0.85	0.85	0.86	0.86	0.90
0.5	0.83	0.83	0.82	0.83	0.83	0.84	0.88
0.6	0.79	0.80	0.79	0.80	0.80	0.81	0.86
0.7	0.76	0.76	0.77	0.81	0.81	0.80	0.83
0.8	0.71	0.70	0.71	0.72	0.71	0.71	0.79
0.9	0.68	0.67	0.66	0.68	0.67	0.68	0.75

**TABLE 11.** Structural Similarity Index (SSIM) of different enhanced images using various algorithms.

Image ID	CLAHE	SSR	ABC	DOCS	CAEN	DCNN	DRF	DHN	Our algorithm
0537	0.85	0.71	0.64	0.56	0.68	0.68	0.66	0.70	0.94
1077	0.91	0.63	0.59	0.61	0.69	0.70	0.66	0.72	0.92
1618	0.76	0.61	0.62	0.59	0.72	0.72	0.69	0.76	0.86
1723	0.86	0.64	0.61	0.53	0.70	0.69	0.68	0.73	0.91
7222	0.78	0.65	0.65	0.65	0.69	0.69	0.67	0.73	0.88
8310	0.92	0.62	0.61	0.57	0.66	0.67	0.64	0.69	0.90
8595	0.87	0.63	0.63	0.58	0.68	0.68	0.67	0.72	0.92
9365	0.89	0.63	0.64	0.62	0.69	0.68	0.66	0.73	0.89
9452	0.90	0.59	0.58	0.59	0.67	0.67	0.66	0.71	0.92

**TABLE 12.** Peak Signal to Noise Ratio (PSNR) of different enhanced images using the networks with different convolution kernel sizes.

Convolution kernel size	$3 \times 3$	$5 \times 5$	$7 \times 7$	$3 \times 3$	$3 \times 3$	$5 \times 5$	$3 \times 3$
Image ID	$3 \times 3$	$5 \times 5$	$7 \times 7$	$5 \times 5$	$7 \times 7$	$5 \times 5$	$5 \times 5$
0537	0.88	0.89	0.88	0.92	0.92	0.91	0.94
1077	0.85	0.84	0.85	0.88	0.89	0.89	0.92
1618	0.80	0.79	0.80	0.83	0.82	0.83	0.86
1723	0.84	0.85	0.84	0.87	0.87	0.88	0.91
7222	0.81	0.81	0.80	0.84	0.85	0.85	0.88
8310	0.84	0.84	0.83	0.86	0.86	0.87	0.90
8595	0.85	0.86	0.85	0.89	0.88	0.88	0.92
9365	0.82	0.83	0.83	0.86	0.87	0.86	0.89
9542	0.85	0.85	0.84	0.88	0.88	0.89	0.92

the worst enhancement effect and the SSIM is the smallest compared with other deep learning based image enhancement algorithms. The DHN can get a good enhancement effect, but compared with the proposed algorithm in this paper, it still has some disadvantages. In general, our algorithm that is proposed in this paper can get the largest SSIM compared with the other algorithms in image enhancement, meaning that it has the best enhancement.

As seen in Table 10, when the attenuation coefficient is small, the convolution kernels of different sizes contributes little to the image enhancement. As the attenuation coefficient increases, the convolution kernels of different sizes play a

role, but the network proposed in this paper can still obtain the best enhancement effect when compared with the algorithms in Table 11.

As shown in Table 11, the image enhanced by the algorithm proposed in this paper can obtain a higher SSIM, which means that the algorithm proposed in this paper has the highest similarity to the original image compared with other algorithms. In other words, the higher the similarity is, the better the enhancement effect is.

As shown in Table 12, the network proposed in this paper which has different convolution kernel sizes can obtain the best enhancement effect, and the results are consistent with

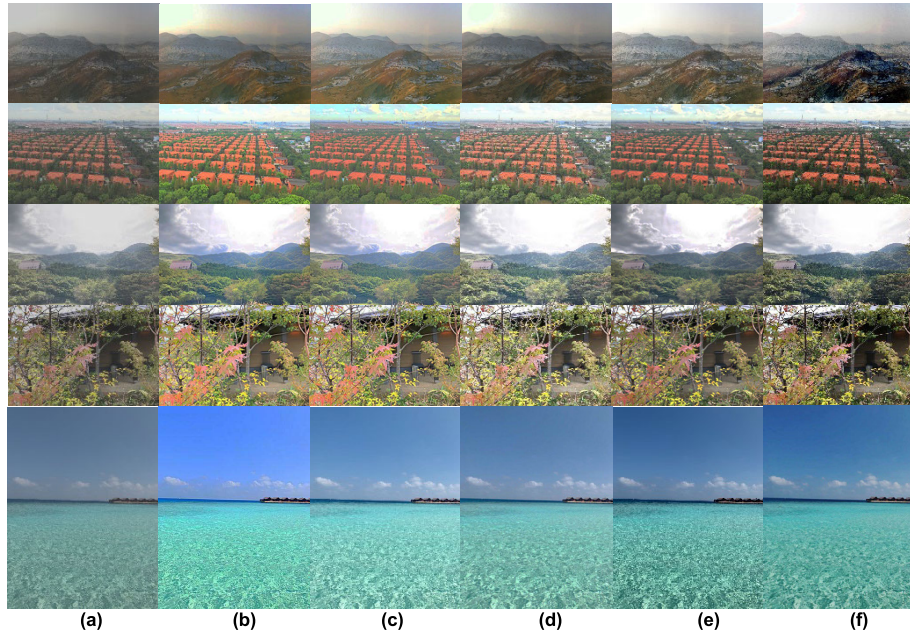


**FIGURE 14.** Enhanced images of different deep learning based image enhancement algorithms.  
 (a) Weak contrast images captured actually, (b) enhanced images using CAEN, (c) enhanced images using DCNN, (d) enhanced images using DRF, (e) enhanced images using DHN, (f) enhanced images using our method.

**TABLE 13.** The Signal to Noise Ratios (SNRs) of enhanced images occupied actually using deep learning based image enhancement algorithms.

Image	CAEN	DCNN	DRF	DHN	Our algorithm
Gobi	31.17	31.25	30.68	32.21	33.48
Houses	31.89	31.95	31.56	32.38	34.24
Scenery	32.21	32.15	30.47	33.29	33.41
Leaves	31.25	31.16	29.46	32.01	32.54
Seaside	30.18	30.24	28.94	31.84	32.49

these in Table 8. In general, ablation experiments show that through changing the size of the convolution kernels, the performance of the network in image enhancement can be improved.

#### E. PERFORMANCE COMPARISON OF DIFFERENT ALGORITHMS ON REAL IMAGES

As discussed above, the deep learning based image enhancement algorithms are superior to traditional image enhancement algorithms. In this section, we further test the effectiveness of the proposed algorithm on the actual captured images. Fig. 14 is the enhanced images of different deep learning based image enhancement algorithms.

As shown in Fig. 14, The CAEN algorithm can significantly improve the brightness of the image, but it cannot enhance image contrast very well, especially when processing the third image. The DCNN algorithm can enhance image contrast to a certain extent, but the effect is generally and the enhancement of DRF algorithm is the worst visually. The DHN algorithm cannot achieve adequate results when processing the first and the fourth images which containing detailed features. Generally speaking, the algorithm proposed

in this paper can ensure that the image is properly handled and also preserve the information of the original image as much as possible.

Since the actual captured images are not the original images, we use the signal-to-noise ratio (SNR) to evaluate the effects of the different algorithms. The SNR of an image should be equal to the power spectrum ratio of the signal to noise, but it is usually difficult to calculate the power spectrum. There is an approximate method to estimate the SNR of images by calculating the ratio of the variance to the mean. The mean of an image can be obtained by as follows:

$$\mu = \frac{1}{M \times N} \sum_x \sum_y f(x, y) \quad (14)$$

where  $M$  is the length of the image,  $N$  is the width of the image, and  $f(x, y)$  is the pixel value at  $(x, y)$ . The variance of an image can be obtained by the following equation.

$$\sigma = \sqrt{\frac{1}{M \times N} \sum_x \sum_y (f(x, y) - \mu)^2} \quad (15)$$

The SNR of an image can be calculated by Equation 25 and the results are given in Table 9.

$$SNR = \frac{\mu}{\sigma} \quad (16)$$

It can be seen from Table 13 that the algorithm proposed in this paper can still simultaneously get the highest Signal to Noise Ratio on actual images and achieve the best image enhancement effect.

## V. CONCLUSION

In this paper, we proposed an improved image enhancement algorithm based on neural networks. This approach analyzes the pixel distribution characteristics of the three channels of weak contrast images. Then, a multi-layer convolution neural network with different convolution kernel sizes is constructed to enhance the weak images, which causes the network to have better feature characterization, and the enhanced images contain better details. Meanwhile, qualitative and quantitative evaluations of a public dataset and the actual obtained images are conducted to evaluate the effectiveness of the algorithm proposed in this paper. Both the contrast experiment and ablation experiment results show that the algorithm proposed in this paper can achieve a higher Peak Signal to Noise Ratio (PSNR) and a higher Structural Similarity Index (SSIM) than other image enhancement algorithms.

## REFERENCES

- [1] M. Yang, J. Hu, C. Li, G. Rohde, Y. Du, and K. Hu, "An in-depth survey of underwater image enhancement and restoration," *IEEE Access*, vol. 7, pp. 123638–123657, 2019.
- [2] W. Kim, R. Lee, M. Park, and S.-H. Lee, "Low-light image enhancement based on maximal diffusion values," *IEEE Access*, vol. 7, pp. 129150–129163, 2019.
- [3] H.-Y. Lin, L.-Q. Chen, and M.-L. Wang, "Improving discrimination in color vision deficiency by image re-coloring," *Sensors*, vol. 19, no. 10, p. 2250, May 2019.
- [4] D. Lee, S. Lee, H. Lee, K. Lee, and H.-J. Lee, "Resolution-preserving generative adversarial networks for image enhancement," *IEEE Access*, vol. 7, pp. 110344–110357, 2019.
- [5] J. Sotelo, J. Urbina, I. Valverde, C. Tejos, P. Irarrazaval, M. E. Andia, S. Uribe, and D. E. Hurtado, "3D quantification of wall shear stress and oscillatory shear index using a finite-element method in 3D CINE PC-MRI data of the thoracic aorta," *IEEE Trans. Med. Imag.*, vol. 35, no. 6, pp. 1475–1487, Jun. 2016.
- [6] W. Liu, P.-H. Yeh, D. E. Nathan, C. Song, H. Wu, G. H. Bonavia, J. Ollinger, and G. Riedy, "Assessment of brain venous structure in military traumatic brain injury patients using susceptibility weighted imaging and quantitative susceptibility mapping," *J. Neurotrauma*, vol. 36, no. 14, pp. 2213–2221, Jul. 2019.
- [7] A. Muthukrishnan, J. C. R. Kumar, D. V. Kumar, and M. Kanagaraj, "Internet of image things-discrete wavelet transform and Gabor wavelet transform based image enhancement resolution technique for IoT satellite applications," *Cogn. Syst. Res.*, vol. 57, pp. 46–53, Oct. 2019.
- [8] A. Manickam, E. Devarasan, G. Manogaran, M. K. Priyan, R. Varatharajan, C.-H. Hsu, and R. Krishnamoorthi, "Score level based latent fingerprint enhancement and matching using SIFT feature," *Multimedia Tools Appl.*, vol. 78, no. 3, pp. 3065–3085, Feb. 2019.
- [9] M. A. Abeed, A. K. Biswas, M. M. Al-Rashid, J. Atulasimha, and S. Bandyopadhyay, "Image processing with dipole-coupled nanomagnets: Noise suppression and edge enhancement detection," *IEEE Trans. Electron Devices*, vol. 64, no. 5, pp. 2417–2424, May 2017.
- [10] Y. Mei and Y. Ning, "Multilayer fusion and chunk-based transmittance estimation for natural hazy image enhancement," *IEEE Access*, vol. 7, pp. 118269–118277, 2019.
- [11] S. Kim, R. Lussi, X. Qu, F. Huang, and H. J. Kim, "Reversible data hiding with automatic brightness preserving contrast enhancement," *IEEE Trans. Circuits Syst. Video Technol.*, vol. 29, no. 8, pp. 2271–2284, Aug. 2019.
- [12] C. Liu, X. Sui, Y. Liu, X. Kuang, G. Gu, and Q. Chen, "Adaptive contrast enhancement based on histogram modification framework," *J. Mod. Opt.*, vol. 66, no. 15, pp. 1590–1601, Sep. 2019.
- [13] J. Jasmine and S. Annadurai, "Real time video image enhancement approach using particle swarm optimisation technique with adaptive cumulative distribution function based histogram equalization," *Measurement*, vol. 145, pp. 833–840, Oct. 2019.
- [14] L. M. Satapathy, R. K. Tripathy, and P. Das, "A combination of variational mode decomposition and histogram equalization for image enhancement," *Nat. Acad. Sci. Lett.*, vol. 42, no. 4, pp. 333–336, Aug. 2019.
- [15] P. Singh, R. Mukundan, and R. De Ryke, "Feature enhancement in medical ultrasound videos using contrast-limited adaptive histogram equalization," *J. Digit. Image*, vol. 157, pp. 1–13, Jul. 2019.
- [16] D. Kasauka, K. Sugiyama, H. Tsutsui, H. Okuhata, and Y. Miyanaga, "An architecture for real-time retinex-based image enhancement and haze removal and its FPGA implementation," *IEICE Trans. Fundam. Electron. Commun. Comput. Sci.*, vol. E102.A, no. 6, pp. 775–782, Jun. 2019.
- [17] C. Tang, U. F. Von Lukas, M. Vahl, S. Wang, Y. Wang, and M. Tan, "Efficient underwater image and video enhancement based on retinex," *Signal Image Video Process.*, vol. 13, no. 5, pp. 1011–1018, Jul. 2019.
- [18] L. Teng, F. Xue, and Q. Bai, "Remote sensing image enhancement via edge-preserving multiscale retinex," *IEEE Photon. J.*, vol. 11, no. 2, Apr. 2019, Art. no. 7000310.
- [19] Q. Sun, H. Jiang, and D. Yi, "A study of pathological image detail enhancement method based on improved single scale retinex," *J. Med. Imag. Health Inform.*, vol. 8, no. 5, pp. 1051–1056, Jun. 2018.
- [20] J. Chen, W. Yu, J. Tian, L. Chen, and Z. Zhou, "Image contrast enhancement using an artificial bee colony algorithm," *Swarm Evol. Comput.*, vol. 38, pp. 287–294, Feb. 2018.
- [21] R. Prasath and T. Kumaran, "Distance-oriented cuckoo search enabled optimal histogram for underwater image enhancement: A novel quality metric analysis," *Imag. Sci. J.*, vol. 67, no. 2, pp. 76–89, Feb. 2019.
- [22] S. Muniyappan and P. Rajendran, "Contrast enhancement of medical images through adaptive genetic algorithm (AGA) over genetic algorithm (GA) and particle swarm optimization (PSO)," *Multimedia Tools Appl.*, vol. 78, no. 6, pp. 6487–6511, Mar. 2019.
- [23] X. Chen, J. Yu, S. Kong, Z. Wu, X. Fang, and L. Wen, "Towards real-time advancement of underwater visual quality with GAN," *IEEE Trans. Ind. Electron.*, vol. 66, no. 12, pp. 9350–9359, Dec. 2019.
- [24] W. L. Wang, X. H. Yang, Y. W. Zhao, N. Gao, C. Lv, and Z. J. Zhang, "Image enhancement algorithm with convolutional auto-encoder network," *J. Zhejiang Univ. Eng. Sci.*, vol. 53, no. 9, pp. 1728–1740, 2019.
- [25] X. Kuang, X. Sui, Y. Liu, Q. Chen, and G. Gu, "Single infrared image enhancement using a deep convolutional neural network," *Neurocomputing*, vol. 332, pp. 119–128, Mar. 2019.
- [26] P. Liu, G. Y. Wang, H. Qi, C. F. Zhang, H. Y. Zheng, and Z. B. Yu, "Underwater image enhancement with a deep residual framework," *IEEE Access*, vol. 7, pp. 94614–94629, 2019.
- [27] W. Ren, S. Liu, L. Ma, Q. Xu, X. Xu, X. Cao, J. Du, and M.-H. Yang, "Low-light image enhancement via a deep hybrid network," *IEEE Trans. Image Process.*, vol. 28, no. 9, pp. 4364–4375, Apr. 2019.
- [28] C. Szegedy, V. Vanhoucke, S. Ioffe, J. Shlens, and Z. Wojna, "Rethinking the inception architecture for computer vision," in *Proc. IEEE Conf. Comput. Vis. Pattern Recognit. (CVPR)*, Jun. 2016, pp. 2818–2826.
- [29] K. Panetta, S. K. M. Kamath, S. Rajeev, and S. S. Agaian, "LQM: Localized quality measure for fingerprint image enhancement," *IEEE Access*, vol. 7, pp. 104567–104576, 2019.
- [30] K. Gu, G. Zhai, W. Lin, and M. Liu, "The analysis of image contrast: From quality assessment to automatic enhancement," *IEEE Trans. Cybern.*, vol. 46, no. 1, pp. 284–297, Jan. 2016.
- [31] W. Y. Li, Y. He, W. Kong, F. Gao, J. Wang, and G. H. Shi, "Enhancement of retinal image from line-scanning ophthalmoscope using generative adversarial networks," *IEEE Access*, vol. 7, pp. 99830–99841, 2019.
- [32] A. Eichenseer, M. Batz, and A. Kaup, "Motion estimation for fisheye video with an application to temporal resolution enhancement," *IEEE Trans. Circuits Syst. Video Technol.*, vol. 29, no. 8, pp. 2376–2390, Aug. 2019.
- [33] E. Protas, J. D. Bratti, J. F. O. Gaya, P. Drews, and S. S. C. Botelho, "Visualization methods for image transformation convolutional neural networks," *IEEE Trans. Neural Netw. Learn. Syst.*, vol. 30, no. 7, pp. 2231–2243, Jul. 2019.

- [34] K. Gu, G. Zhai, X. Yang, W. Zhang, and C. Wen Chen, "Automatic contrast enhancement technology with saliency preservation," *IEEE Trans. Circuits Syst. Video Technol.*, vol. 25, no. 9, pp. 1480–1494, Sep. 2015.
- [35] H.-T. Wu, W. Mai, S. Meng, Y.-M. Cheung, and S. Tang, "Reversible data hiding with image contrast enhancement based on two-dimensional histogram modification," *IEEE Access*, vol. 7, pp. 83332–83342, 2019.
- [36] W. Zhao, D. Wang, and H. Lu, "Multi-focus image fusion with a natural enhancement via a joint multi-level deeply supervised convolutional neural network," *IEEE Trans. Circuits Syst. Video Technol.*, vol. 29, no. 4, pp. 1102–1115, Apr. 2019.
- [37] B.-H. Chen, Y.-L. Wu, and L.-F. Shi, "A fast image contrast enhancement algorithm using entropy-preserving mapping prior," *IEEE Trans. Circuits Syst. Video Technol.*, vol. 29, no. 1, pp. 38–49, Jan. 2019.
- [38] Y. Liu, Z. Qin, and J. H. Wu, "Cryptanalysis and enhancement of an image encryption scheme based on bit-plane extraction and multiple chaotic maps," *IEEE Access*, vol. 7, pp. 74070–74080, 2019.
- [39] S.-Y. Yu and H. Zhu, "Low-illumination image enhancement algorithm based on a physical lighting model," *IEEE Trans. Circuits Syst. Video Technol.*, vol. 29, no. 1, pp. 28–37, Jan. 2019.
- [40] Y. Su, W. Sun, J. Liu, G. Zhai, and P. Jing, "Photo-realistic image bit-depth enhancement via residual transposed convolutional neural network," *Neurocomputing*, vol. 347, pp. 200–211, Jun. 2019.
- [41] K. Gu, D. Tao, J.-F. Qiao, and W. Lin, "Learning a no-reference quality assessment model of enhanced images with big data," *IEEE Trans. Neural Netw. Learn. Syst.*, vol. 29, no. 4, pp. 1301–1313, Apr. 2018.
- [42] L. Huang, W. Zhao, B. R. Abidi, and M. A. Abidi, "A constrained optimization approach for image gradient enhancement," *IEEE Trans. Circuits Syst. Video Technol.*, vol. 28, no. 8, pp. 1707–1718, Aug. 2018.
- [43] L. Lin, D. Wang, S. Zhao, L. Chen, and N. Huang, "Power quality disturbance feature selection and pattern recognition based on image enhancement techniques," *IEEE Access*, vol. 7, pp. 67889–67904, 2019.
- [44] K. Gu, W. Lin, G. Zhai, X. Yang, W. Zhang, and C. W. Chen, "No-reference quality metric of contrast-distorted images based on information maximization," *IEEE Trans. Cybern.*, vol. 47, no. 12, pp. 4559–4565, Dec. 2017.
- [45] Accessed: Jun. 15, 2018. [Online]. Available: <https://pytorch.org/>



**JIAO WANG** was born in Xinyi, Jiang Su, China, in 1992. He received the B.S. and M.S. degrees in communication engineering from Beijing Information Science and Technology University, in 2013 and 2016, respectively. He is currently pursuing the Ph.D. degree with the Beijing Key Laboratory of Work Safety Intelligent Monitoring, School of Automation, Beijing University of Posts and Telecommunications. His research interests include computer vision and image processing.



**YANZHU HU** was born in Beijing, China, in 1970. He received the B.S. degree in control science and engineering from the Beijing University of Aeronautics and Astronautics, in 1991, the M.S. degree in economic management from the Chinese Academy of Social Sciences, in 1997, and the Ph.D. degree in systems engineering from Beijing Jiaotong University, in 2005. From 2006 to 2007, he did his Postdoctoral Research at Beijing Jiaotong University.

Since 2008, he has been a Professor with the School of Automation, Beijing University of Posts and Telecommunications. He is the author of more than 15 articles. His research interests include intelligent monitoring and image processing.

• • •